ACS POLYMERS Au
AN OPEN ACCESS JOURNAL OF THE AMERICAN CHEMICAL SOCIETY

pubs.acs.org/polymerau
Article

Clickable Polyprolines from Azido-proline *N*-Carboxyanhydride

Published as part of the ACS Polymers Au virtual special issue "2023 Rising Stars".

Rachel E. Detwiler, Thomas J. McPartlon, Clara S. Coffey, and Jessica R. Kramer*

Cite This: *ACS Polym. Au* 2023, 3, 383–393
Read Online

ACCESS | Metrics & More | Article Recommendations | Supporting Information

ABSTRACT: Polyproline is a material of great interest in biomedicine due to its helical scaffold of structural importance in collagen and mucins and its ability to gel and to change conformations in response to temperature. Appending of function-modulating chemical groups to such a material is desirable to diversify potential applications. Here, we describe the synthesis of high-molecular-weight homo, block, and statistical polymers of azide-functionalized proline. The azide groups served as moieties for highly efficient click-grafting, as stabilizers of the polyproline PPII helix, and as modulators of thermoresponsiveness. Saccharides and ethylene glycol were utilized to explore small-molecule grafting, and glutamate polymers were utilized to form polyelectrolyte bottlebrush architectures. Secondary structure effects of both the azide and click modifications, as well as lower critical solution temperature behavior, were characterized. The polyazidoprolines and click products were well tolerated by live human cells and are expected to find use in diverse biomedical applications.

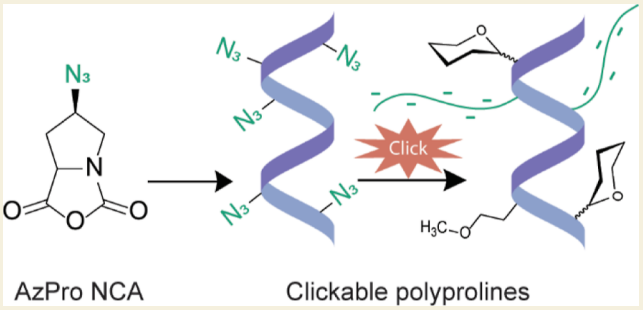

KEYWORDS: *polyproline, PPII, polypeptide, glycopolypeptide, N-carboxyanhydride*

INTRODUCTION

Proline-rich proteins are among the most conserved structures in animals. Proline (Pro) is essential for the structure of collagen,[1] the most abundant protein in the human body, as well as mucus,[2] which is highly conserved across diverse species. Pro is a unique amino acid in that its sidechain is a 5-membered ring that wraps back to the nitrogen atom. When in peptides, the Pro nitrogen lacks a proton and therefore cannot participate in hydrogen bonds. Dense runs of Pro induce a highly ordered left-handed helical conformation, which surely drives biomolecular functions and recognition processes.[3,4]

Synthetic polyPro (PPro) is a material of great interest since it adopts the left-handed helical conformation, termed a PPro II (PPII) helix. The PPII helix contains 3 residues per turn.[5] PPro can also adopt a PPI helical structure that is more compact with 3.3 residues per turn (Figure 1A).[5] Due to the ring structure and allowed peptide backbone dihedral angles, the equilibrium between cis and trans peptide conformations is more favorable than for any other amino acid (Figure 1B).[6] The PPI helix contains predominantly cis peptide bonds and is favorable in organic solvents, while the PPII helix contains predominantly trans bonds and is favorable in water.[7−12] Synthetic PPro has been essential for probing the propensity and equilibria of such structures.[13]

PPro is of interest in biomedical applications and has been utilized as a molecular ruler,[14] in hydrogel formulation,[15] affinity purifications,[16] anti-thrombotics,[17] cryoprotectants,[18] and in collagen mimics.[1,19] Considering the diverse applications, it is desirable to display functional or bioactive groups to induce biological interactions or modulate properties of PPro. Further, the PPII helix presents an opportunity to probe binding events from an ordered and natural scaffold.

Here, we describe the synthesis of clickable PPro that enables rapid functionalization with groups of interest. The click reactions proceed with high efficiency and even allow grafting-to brush preparation.

The major route to high molecular weight (MW) polypeptides is by polymerization of α-amino acid *N*-carboxyanhydrides (NCAs).[20] The method is rapid, scalable, and highly tunable. Two routes to functionalized polypeptides are possible: polymerization of a functionalized NCA monomer or post-polymerization modification.[21−23] Post-polymerization modifications are generally synthetically more straightforward. However, the reaction toolbox is limited to fairly benign conditions, and achieving high degrees of functionalization is challenging due to steric hindrance. Incomplete modification results in leftover reactive chemical

Received: May 1, 2023
Revised: June 29, 2023
Accepted: June 30, 2023
Published: July 16, 2023

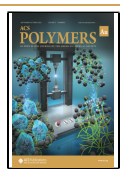

https://doi.org/10.1021/acspolymersau.3c00011
ACS Polym. Au 2023, 3, 383−393

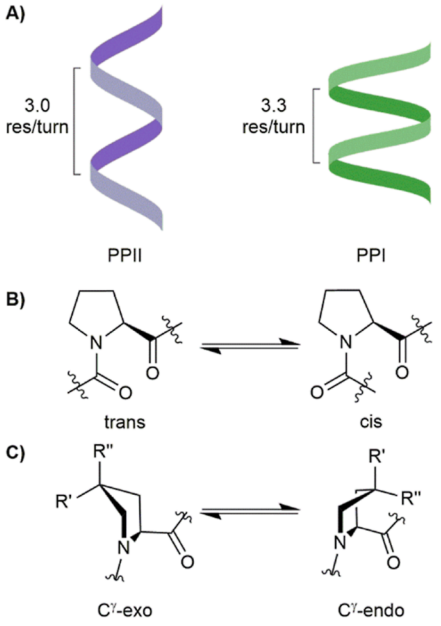

Figure 1. (A) Extended PPII helix with 3 residues per turn and 9.3 Å helical pitch vs compact PPI helix with 3.3 residues per turn and 6.3 Å helical pitch; (B) *trans* vs *cis* L-Pro peptide bonds where PPII structures are predominantly trans and PPI are predominantly cis; (C) ring pucker conformations of 4-substituted L-Pro where 4*R* stereochemistry results in substituents at R′ (i.e., Hyp or Azp, R′ = OH or N_3; R″ = H).

groups that may be undesirable. The functionalized monomer route is attractive in that the plethora of small molecule chemistries can be utilized and functionalization degrees of up to 100% are possible. The drawback is optimizing a new monomer and preparing individual polymers for each desired functional group. Polypeptides bearing clickable groups offer a nice hybrid option where the development of a single monomer and polymer structure opens the door to many desired products.[21,22]

Clickable polypeptides have been an area of recent interest, and a broad array of chemistries have been utilized, including thiol-ene/yne reactions,[21] methionine sulfoniums,[24] and azide−alkyne cycloadditions.[21−23] Azide−alkyne cycloaddition reactions are particularly attractive due to their rapid kinetics, small molecular size, ease of installation, and many commercially available reagents. Interestingly, despite a plethora of published alkyne-functionalized NCAs and polypeptides, we could find only a single report of an azide-functionalized monomer derived from lysine/ornithine[25] and a single PPM-derived azido-polypeptide based on glutamic acid.[26] In both cases, a classic right-handed α-helix was adopted for both the parent and click-functionalized polypeptides. Wennemers and co-workers prepared azide-modified Pro amino acids[27] and short peptides.[28] However, to our knowledge, there have been no reports of the preparation of high MW, readily tunable, scalable, and clickable PPII polymeric scaffolds.

We investigated azide-functionalized PPro since preparation of the amino acid is straightforward and conducive to multigram scale synthesis. Additionally, Wennemers et al. reported the conformational effects of the azide as favoring transpeptide bonds and stabilizing the PPII secondary structure.[27,28] Here, we report the synthesis and controlled polymerization of azido-Pro (Azp) NCA to yield high MW polypeptides that were ready substrates for click-functionalization (Scheme 1A−E). We used these materials as scaffolds for the presentation of sugars and ethylene glycol (EG) and to prepare polyelectrolyte brushes. We also demonstrate that the materials are non-toxic to human cells, further indicating they are ripe for biomedical applications.

RESULTS AND DISCUSSION

We prepared (2*S*,4*R*)-4-azido-L-Pro (Azp) from commercially available (2*S*,4*R*)-hydroxyPro (Hyp). Hyp is the most common post-translational modification in animals and is enzymatically generated solely with 4*R* stereochemistry.[29] The *R* configuration puts the appended hydroxyl on the face of the pyrrolidine ring opposite from the carboxyl group.[30] Studies by Raines and co-workers propose that the resulting gauche effect of electron withdrawing groups enables an n → π^* interaction between nonbonding OH electrons and the peptide carbonyl, which stabilizes the C$^{\gamma}$-exo ring pucker and promotes equilibria toward the trans peptide bond (Figure 1C).[31] This effect has consequences for the structural stability of proteins such as collagen, and indeed, non-native (2*S*,4*S*)-Hyp has been shown to destabilize the collagen triple helix.[32]

The Wennemers laboratory studied Azp in the context of capped amino acids and short peptides. They reported a 2.3-fold preference for the trans peptide bond for Ac-(4*R*)-Azp-OMe as compared to Ac-(4*S*)-Azp-OMe.[27] The equilibria were proposed to be driven by a Hyp-reminiscent n → π^* interaction between the nonbonding electrons of the terminal *N*-acetyl oxygen and the ester carbonyl. Later, they studied Pro 9-mers with 4*R* vs 4*S* azides and reported that in organic/aqueous cosolvents, the PPII helix was stabilized by (4*R*)-Azp and destabilized by (4*S*)-Azp.[28] As there was no *N*-acetyl group present, the effect was rationalized based on work by Horng and Raines on 4*R* vs 4*S* 4-fluoroPro 10-mers.[33] Raines indicated that electron-withdrawing 4*R* substituents stabilize the PPII helix relative to PPI, even in solvents that favor the PPI conformation. 4*S*-Azp is simpler to prepare, but based on this collective data, we pursued the synthesis and polymerization of Azp NCA with native 4*R* stereochemistry.

Following a literature protocol,[34] commercially available *tert*-butyloxycarbonyl-(2*S*,4*R*)-Hyp (Boc-Hyp) was converted to the methyl ester, and 4-hydroxy stereochemistry was inverted to *S* by an intramolecular Mitsunobu reaction followed by methanolysis (Scheme 1A). To install the 4*R* azide group, 4*S*-Hyp-OMe was treated with diphenylphosphoryl azide under Mitsunobu conditions. The resulting (2*S*,4*R*)-Az-Pro-OMe was hydrolyzed to the free acid and then converted to Azp NCA by treatment with triphosgene and triethylamine using optimized conditions for Pro NCA preparation.[13,35,36] The Boc-protecting group was utilized since prior work by our laboratory and others on the preparation of Pro NCA revealed higher yielding cyclization from the Boc-protected amino acid as compared to cyclization of Pro. Highly pure crystalline monomer was obtained after anhydrous flash column chromatography on silica,[37] and the NCA was stored under an inert atmosphere to prevent hydrolysis and premature polymerization.

In an effort to optimize Azp polymerization, we explored two ring-opening polymerization (ROP) methods (Scheme 1A,D). We utilized our previously reported transition metal initiators that proceed under inert atmosphere conditions,[13] or water-assisted, amine-initiated ROP that proceeds in an open atmosphere.[38] Transition metal initiated ROPs typically

https://doi.org/10.1021/acspolymersau.3c00011
ACS Polym. Au 2023, 3, 383−393

Scheme 1. (A) Synthesis of Azp, Conversion to Azp NCA Monomer, and Two ROP Routes to polyAzp; DIAD = Diisopropyl Azodicarboxylate, PPh_3 = Triphenylphosphine, MeOH = Methanol, DPPA = Diphenylphosphoryl Azide, DEAD = Diethyl Azodicarboxylate, TEA = Triethylamine; (B) Preparation of Statistical Copolypeptides by Pre-mixing of NCAs Followed by Treatment with Ni Initiator (Copolymers with BnGlu Are Not Pictured); (C) Preparation of Block Copolypeptides by Sequential Addition of NCAs after Treatment with Co Initiator; (D) Structures of Initiators Used in This Study; (E) Cartoon Representation of Clickable PPro

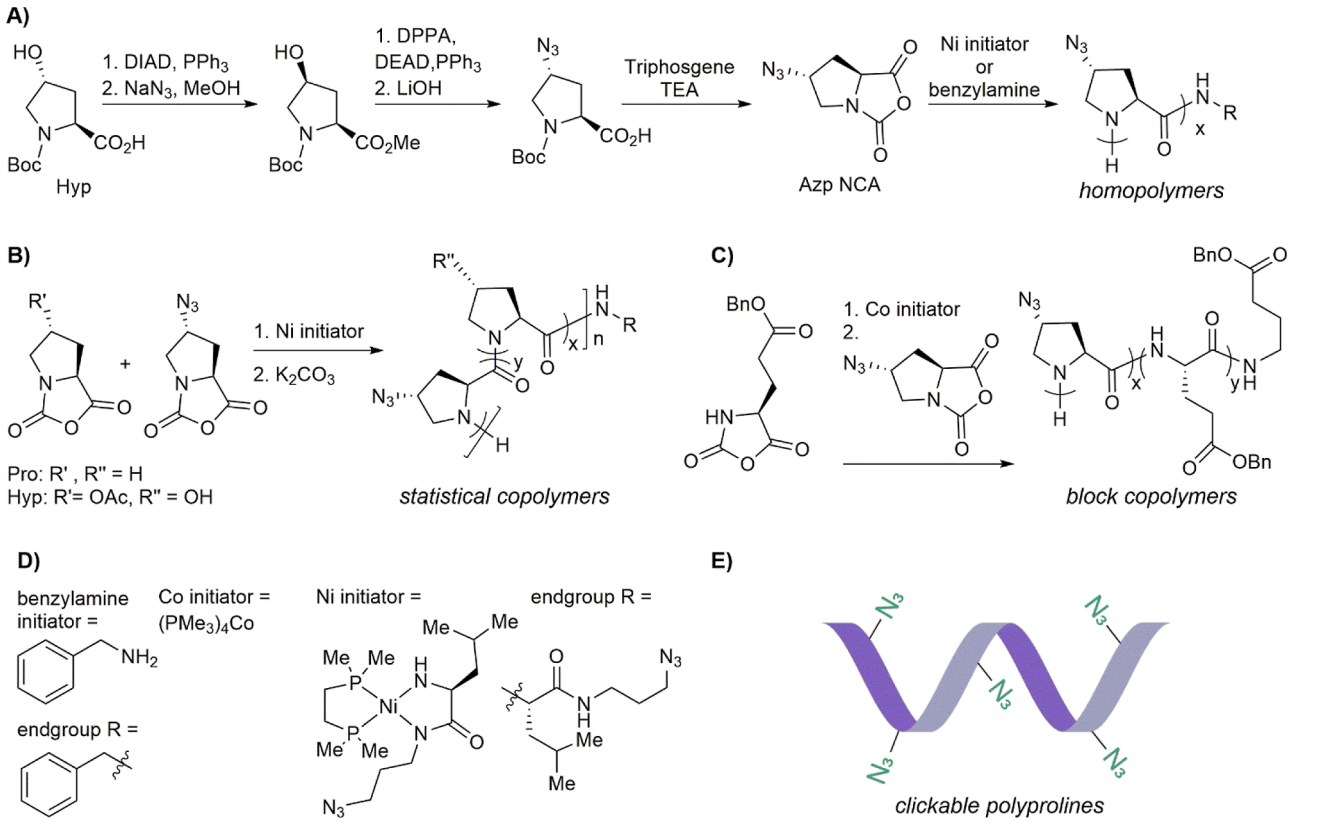

complete in a few hours, can achieve high degrees of polymerization (DPs) (i.e., DP = ~500) with excellent MW control, have low dispersities (*Đ*s), and have living conditions where multiblock structures can be prepared.[20,39] Classic amine-initiated polymerizations take up to a week to complete, result in lower DPs (i.e., DP = ~30), higher dispersities (*Đ*s), and are not living. However, in recent years, many advances have been made to overcome these challenges.[40−42] One such example is in a recent report by Lu and co-workers who developed a water-assisted variation (typically 1:1 water/acetonitrile) that proceeds in minutes with good MW control for a variety of NCAs.[35] We rationalized that water-mediated polymerization might avoid the multi-day PPI to PPII conversion after metal-catalyzed Pro polymerizations conducted in organic solvents.

We prepared homopolymers of Azp (PAzp) at varied monomer-to-initiator ratios ([M]/[I]s) using our Ni initiator in dimethylformamide (DMF) or tetrahydrofuran (THF). In all cases, the reaction resulted in the complete consumption of monomer, as evidenced by attenuated total reflectance Fourier transformed infrared spectroscopy (ATR−FTIR) (Figure 2A) and the formation of polymeric organogels. Gelation impeded direct analysis of the homopolymers by size exclusion chromatography coupled to multi-angle light scattering and refractive index detectors (SEC/MALS/RI) since our system runs with DMF. We could, however, prepare DMF-soluble diblock copolymers using poly-γ-benzyl-L-glutamate (PBnGlu) as a macroinitiator (Scheme 1C).

Macroinitiators were prepared by polymerization of BnGlu NCA using Co initiator in THF using previously reported conditions.[43] An aliquot was analyzed by SEC/MALS/RI to be $BnGlu_{73}$, M_n = 15,710, *Đ* = 1.192. The DP and M_n from an [M]/[I] of 25:1 were as expected based on the known cobalt initiator efficiency.[44] After conversion to $BnGlu_{73}$, the living chain end was used to initiate polymerization of Azp NCA at varied [M]/[I]s. The products were analyzed by ^1H NMR, and $BnGlu_{73}$ was used as an internal NMR standard. Linear chain growth was observed for PAzp, and MWs aligned well with predicted values (Figure 2B and Table 1). From these data, we can infer that Azp NCA, like many other NCAs, can undergo transition-metal-mediated polymerization in a highly controlled manner.

Upon first dissolution in water, PPro is in its insoluble PPI form, which slowly (~5 days) equilibrates to the thermodynamically favored soluble PPII form.[13] PAzp dispersions at 0.5 or 1 mg/mL, however, remained cloudy for the 3 week period we examined. Centrifugation and separate lyophilization of the soluble and insoluble fractions revealed that only 26% of the material was soluble. Dissolution of the soluble fraction resulted in a solution that was again cloudy, indicating that PAzp is likely in conformational equilibrium.

Attempts to solubilize PAzp in a variety of solvents (THF, CH_2Cl_2, $CHCl_3$, MeOH, *n*-propanol, acetonitrile, and water)

https://doi.org/10.1021/acspolymersau.3c00011
ACS Polym. Au 2023, 3, 383−393

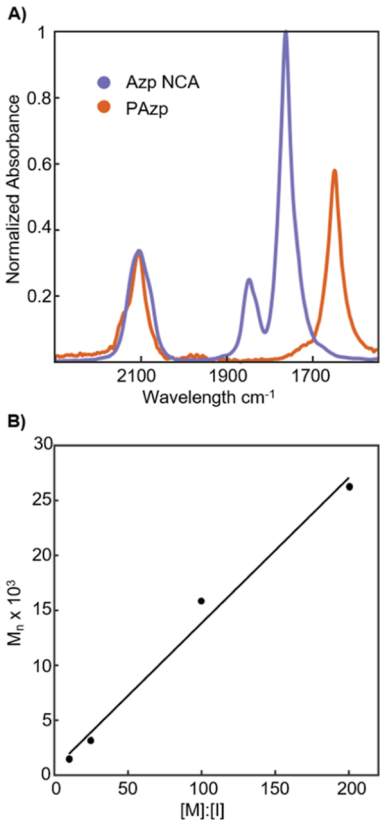

Figure 2. (A) ATR−FTIR data for conversion of Azp NCA to PAzp with intact azide group using Ni initiator in DMF at ambient temperature. (B) Polymerization data for growth of PAzp chains from a $BnGlu_{73}$ macroinitiator indicating controlled polymerization; M_n is for the PAzp segment, R^2 = 0.9872.

Table 1. Representative Polymerization Data

polymer[a]	[M]/[I][b]	initiator	M_n	$Đ$[g]
Azp_{16}	25	benzyl amine[c]	2210[g]	N.D.
Azp_{21}	50	benzyl amine[c]	2901[g]	N.D.
Azp_{18}	100	benzyl amine[c]	2847[g]	N.D.
$BnGlu_{73}$[d]	25	Co initiator	15,710	1.19
Azp_{11}[f]	10	$BnGlu_{73}$[d]	1529[g,i]	N.D.
Azp_{24}[f]	25	$BnGlu_{73}$[d]	3267[g,i]	N.D.
Azp_{114}[f]	100	$BnGlu_{73}$[d]	15,790[g,i]	N.D.
Azp_{190}[f]	200	$BnGlu_{73}$[d]	26,202[g,i]	N.D.
Azp_{15}-*s*-$AcOPro_{45}$	50	Ni initiator[e]	9467[h]	1.30[h]
$GalTzp_{35}$[j]			31,030[h]	1.02[h]
$GalTzp_{15}$-*s*-$AcOPro_{45}$[j]			20,030[h]	1.20[h]
$GalTzp_{15}$-*s*-$AcOPro_{45}$[j]			37,540[h]	1.07[h]

[a]Sample name and observed polypeptide DP. [b]Molar ratio of NCA to initiator. [c]Polymerization performed in 5% water in DMSO. [d]Polymerization performed in THF. [e]Polymerization performed in DMF. [f]Samples were analyzed as block polymers $BnGlu_{73}$-*b*-Azp_x for improved solubility. [g]M_n or $Đ$ as determined by ^{1}H NMR in DMSO. [h]M_n or $Đ$ as determined by SEC/MALS/RI; $Đ$ could not be determined (N.D.) in cases where the polypeptide was poorly soluble in DMF. [i]M_n reported is for the PAzp segments only and does not include the macroinitiator. [j]SEC/MALS/RI analysis was performed after click-conjugation.

revealed that dimethylsulfoxide (DMSO) was by far the most efficient solvent for this compound. Therefore, we used water/DMSO mixtures to explore water-assisted amine-initiated ROP.[35] We conducted polymerizations using benzyl amine at [M]/[I]s from 10 to 100 and at varied percentages of water in DMSO. In 5% water in DMSO, NCA was consumed within 30 min, and the resulting PAzp formed an organogel. Using the benzyl group protons and ^{1}H NMR analysis, we obtained the MWs of the PAzps formed in DMSO with 5% water. We observed a plateau effect where polymers did not grow past ca. 20 residues, presumably due to gelation rendering chain ends inaccessible (Table 1). Attempts to use less water and circumvent gel formation resulted in slow polymerization kinetics and associated poor conversion of NCA to polypeptide. By contrast, when reacted at [100]:[1] with benzylamine in DMSO with 50 or 2% water 2*S*,4*R*-acetoxyPro (AcOPro) NCA was fully consumed in under 2 min and yielded a 125-mer.

Overall, we found homopolymers of PAzp challenging to work with due to their organogelation propensity. Previous work on lysine/ornithine-derived azide-functionalized homologs of norvaline and norleucine was also noted to have poor solubility,[25] so we presume this to be an inherent property of polypeptides with a high density of this chemical motif. However, DMSO is a suitable solvent for many purposes, and for the application as a scaffold for the display of functional groups, homopolypeptides are typically not necessary and copolypeptides are desirable.

To serve as scaffolds for proof-of-concept for click reactions and to probe polypeptide secondary structures, we prepared statistical copolymers of Azp with BnGlu, Pro, and AcOPro, which are deacetylated to yield Hyp (Scheme 1B). Copolypeptides were achieved by pre-mixing Azp and BnGlu, Pro, or AcOPro NCAs at ratios of 1:3 or 1:1, followed by treatment with the Ni initiator. NCA was rapidly consumed, and as copolymers, no gelation was observed, and solubility in THF and DMF was greatly improved as compared to PAzp homopolymers. We did not obtain kinetic data for Azp NCA; however, our previous work on Pro and N-substituted NCA polymerizations indicates the structures are not likely to be tapered.[13,45] Copolymers containing AcOPro were readily deprotected by overnight treatment with K_2CO_3 in methanol/water, and those with BnGlu were deprotected with trimethylsilyliodide in dichloromethane. All copolymers were purified by dialysis or spin-filtration with Milli-Q water and were fully water soluble.

We used circular dichroism (CD) spectroscopy to investigate the secondary structures of the various polypeptides. CD relies on the absorption of light by peptide bonds. The wavelengths at which the absorptions occur and their intensities reveal characteristics about the orientation and energetics of those bonds. In organic solvents, PPro adopts a PPI structure, while in aqueous solutions, it eventually equilibrates to PPII.[13,33] PHyp's aqueous form is also PPII. PolyGlu (PGlu), which is obviously lacking Pro residues, also adopts a PPII-like conformation due to the high density packing of charged groups, causing extension and rigidification of the peptide backbone.[46,47] The notion of the adoption of PPII conformations by molecules lacking Pro was initially not readily accepted.[48] However, subsequent studies have offered strong evidence, and the PPII helix is now known to be an important conformation adopted by charged polypeptides as well as diverse proteins and peptides.[49−51] PPI and PPII can be easily differentiated by their absorption ellipticities. The PPI n → π^* results in a moderately negative minimum at ∼230 nm and the $\pi \rightarrow \pi^*$ a strong maximum at ∼212 nm. The PPII form has a minor positive maximum at ∼226 nm and a strong

https://doi.org/10.1021/acspolymersau.3c00011
ACS Polym. Au 2023, 3, 383−393

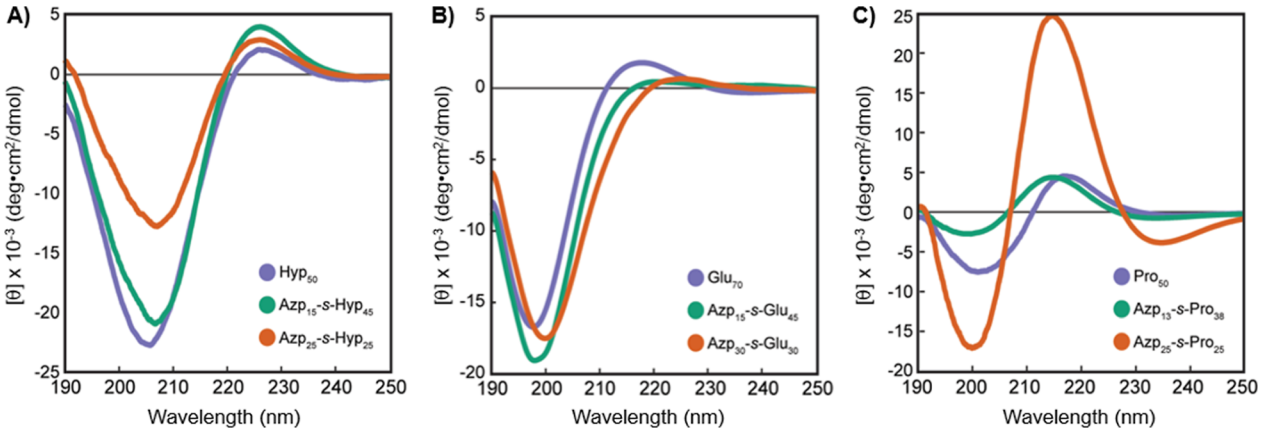

Figure 3. CD spectra at 20 °C of (A) PHyp and statistical copolymers of Hyp and Azp in water; (B) PGlu and statistical copolymers of Glu and Azp in water; and (C) PPro and statistical copolymers of Pro and Azp in 95% *n*-propanol 5% water.

negative minimum at ∼206 nm (218 and 197 nm for PGlu).[13,50]

Prior CD work on Pro and Azp 9-mers indicates that in n-propanol, the peptides adopt the PPI conformation.[28,33] The addition of just 5% water sufficiently hydrated the peptide backbones to observe a mix of PPI and PPII. CDs of 4*R* vs 4*S* Azp 9-mers in solutions of decreasing n-propanol content indicated that 4*R*-Azp$_9$ adopts the PPII structure at a lower water content than 4*S*. This was interpreted to mean that the 4*R* azide has a stabilizing effect on the PPII helix and the 4*S* azide has a destabilizing effect, at least relative to one another.

Considering the PPII and PPI helices contain 3 and 3.3 residues per turn, respectively, an Azp 9-mer can only make 2−3 helical turns, and that assumes the terminal residues are well-behaved. Higher MW PAzps should be explored to better understand conformational effects. Indeed, our own work on Pro and Hyp has shown that the CD spectra of 10-mers differ from those of 25-mers, but that the structure changes little after that length.[13] It is well known that in CD spectra, the per-residue dichroism increases with chain length and molecular stiffness.[52,53] Additionally, observation of the perturbing effects of Azp on known secondary structures has not been explored. Therefore, we investigated 50-mers that can make 15−16 helical turns and with increasing Azp ratios in copolymers with Pro, Hyp, and Glu.

Introduction of Azp residues to PPII-former PHyp resulted in an increase in intensity for signature n → π^* ellipticities at ca. 226 nm (Figure 3A). Substitution with 25% Azp (Azp$_{15}$-*s*-Hyp$_{45}$) resulted in a greater increase than that of a 50/50 blend (Azp$_{25}$-*s*-Hyp$_{25}$). The $\pi \rightarrow \pi^*$ absorbance was strongly reduced for the 50% Azp polymer but not for the 25% Azp structure. We suspect that the poorer water solubility of the Azp residues is at play and interaction with water molecules affects the energetics of the $\pi \rightarrow \pi^*$ transition.

The PPII-like extended conformation of PGlu appeared to relax slightly due to the introduction of 25 or 50% Azp (Azp$_{15}$-*s*-Glu$_{45}$, Azp$_{30}$-*s*-Glu$_{30}$) since the intensity of the n → π^* was reduced (Figure 3B). Charge repulsion is likely the dominant force since spacing the anionic groups resulted in the minor relaxation. As expected, we also observed a red-shift with increasing tertiary amide content.[46,47,50] The $\pi \rightarrow \pi^*$ absorbance was less affected, corroborating the hypothesis that water molecules, bound in this case by charged sidechains, play a role in this energetic transition.

We sought to examine the effect of Azp on PPI structure by examining 25 or 50% copolymers with Pro (Azp$_{13}$-*s*-Pro$_{38}$ and Azp$_{25}$-*s*-Pro$_{25}$) in organic solvent. Azp and Pro 9-mers were reportedly soluble in *n*-propanol;[28] however, none of our Azp-containing 50-mers would dissolve (nor Pro$_{50}$ or Pro$_{25}$). Our polymers were, however, soluble in n-propanol with 5% water and were incubated in this solvent for 2 days prior to obtaining spectra. As expected, the obtained Pro$_{50}$ CD spectrum indicated a mixture of PPI and PPII conformations, as noted by the shifted maximum at 217 nm and minimum at 201 nm as compared to pure PPII (Figure 3C). The maximum for 25% Azp (Azp$_{13}$-*s*-Pro$_{38}$) was further shifted to 214 nm and the minimum to 200 nm. Increased Azp content to 50% (Azp$_{25}$-*s*-Pro$_{25}$) resulted in an increase in ellipticity but no further shift in absorbance wavelength. Apparently, in organic solvents, the Azp group drives the equilibrium toward PPI. The Azp polymer data were unexpected considering that in aqueous solvent stabilization of PPII was observed. Presumably, hydration plays a bigger role in PPII stabilization than the electron withdrawing effects of the 4*R* azide group.

Proper CD of PAzp homopolymers could not be obtained due to poor water and alcohol solubility as previously described, and since DMSO (which is a good solvent) absorbs in the same region as the peptide amides. However, a small fraction of PAzp forms a water-soluble equilibrium component. Therefore, we centrifuged away the insoluble polymer and analyzed the remaining soluble fraction by CD. Concentration was determined by Beer's law. Data indicated a lower PPII helical propensity for Azp$_{90}$ than for Pro$_{100}$ (Figure S1). However, considering the homopolymer solubility challenges, we consider the copolymer data more informative.

PPro has an aqueous lower critical solution temperature (LCST) where the polymer is miscible with water below the LCST, but above the LCST aggregation occurs, resulting in two immiscible phases in thermodynamic equilibrium.[54] I.e., above the LCST temperature, polymer solutions become cloudy. The cloud point temperature (T_{CP}) of PPro is ca. 67 °C, depending on length and potentially on the polymer endgroup.[54] A conformational shift from PPII to PPI is implicated as a driver of this process.

We investigated the effect of the 4*R* Az group on PPro's T_{CP}. We first confirmed if there were any effects of chain length or end group in our own hands. PPro 50- or 100-mers were prepared via water-assisted amine polymerizations using hexyl-, 2-methoxyethyl-, or cholestryl-amines as initiators to tune end-

https://doi.org/10.1021/acspolymersau.3c00011
ACS Polym. Au 2023, 3, 383−393

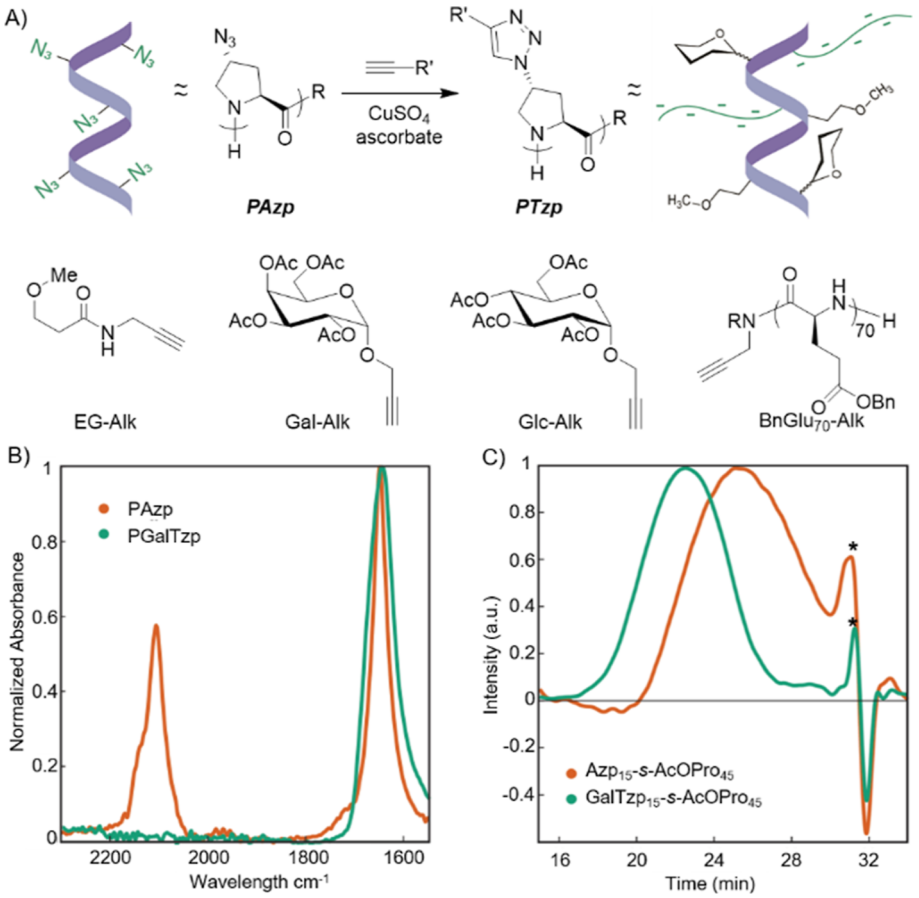

Figure 4. (A) Copper-catalyzed cycloadditions of helical Azp-polypeptides and alkyne-functionalized EG, Gal, Glc, and polyelectrolyte brush precursor PBnGlu. (B) ATR−FTIR absorbance spectra, normalized to the amide peak at ∼1650 cm^{-1}, for Azp_{35} before and after the click reaction with Gal-Alk. (C) SEC/MALS/RI analysis of Azp_{15}-*s*-$AcOP_{45}$ before and after click reaction with Gal-Alk (* denotes the solvent signal).

group size and hydrophobicity. Polypeptide solutions at 5 mg/mL were heated at a rate of 1 °C per minute from 10 to 95 °C and were monitored spectroscopically at 600 nm. The T_{CP} shifted only slightly with chain length from 68 to 73 °C for Pro_{50} vs Pro_{100}. Varied end-groups on Pro_{100}-mers also had little effect on T_{CP} (see Supporting Information, Table S1). Therefore, we examined varied polymer compositions with 4*R* substituents as 100-mers and with hexylamine end-groups.

Substitution of 10% of $PPro_{100}$'s residues with Azp (Azp_{10}-*s*-Pro_{90}) resulted in a T_{CP} of 81 °C, an 8 °C increase from Pro_{100}. Interestingly, substitution with AcOPro ($AcOPro_{10}$-*s*-Pro_{90}) had no effect, and the T_{CP} remained at 73 °C. Substitution with 25% Azp (Azp_{25}-*s*-Pro_{75}) resulted in a loss of LCST, while 25% AcOPro's ($AcOPro_{25}$-*s*-Pro_{75}) T_{CP} shifted by only 5 °C. Hyp polypeptides had no observable LCST. Complete LCST data can be found in Table S1.

Presumably, the effects of the 4*R* hydroxy and azide groups on PPro's LCST are due to stabilization of the PPII helix via their electron withdrawing effects, resulting in n → π^* interactions that shift the preference for *trans* vs *cis* amides; i.e., increasing stabilization increases the LCST. The 4*R* acetoxy group, which is moderately donating, had far less effect on T_{CP}. Hydrophilicity and water-binding capacity might also be at play. Overall, these data concur with the CD data indicating stabilization of the aqueous PPII helix by the 4*R* Az group.

We utilized both homo- and co-polymers of Azp as ordered helical scaffolds from which to append functional groups using copper click chemistry (Figure 4A). We chose monomethyl EG, galactose (Gal), and glucose (Glc) as small molecules and PGlu as a macromolecule with which to form polyelectrolyte brushes (Figure 4A). EG and PGlu are widely used structures in biomedicine[55,56] while Gal and Glc are useful as non-ionic, hydrophilic groups that have innate bioactivity.[57] Additionally, these cases allow for exploration of conjugation efficiency to the helical PAzp scaffold. EG is relatively small in molecular size for ease of grafting reactions; Gal/Glc are sterically more demanding; and PGlu is an even more challenging case where bottlebrush preparation is typically difficult to achieve with high grafting density. To further probe reaction grafting efficiency and tune material properties, we selected two clickable backbone substrates: copolymer Azp_{15}-*s*-$AcOPro_{45}$, which spaces available click groups, and homopolymer Azp_{35}, where azide groups are maximally packed.

Alkyne-functional EG, Gal, and Glc, (EG-Alk, Gal-Alk, and Glc-Alk, Figure 4B), were readily synthesized via published procedures.[58,59] Saccharides were utilized in their peracetylated forms. $BnGlu_{70}$ was prepared by water-assisted polymerization of BnGlu NCA using propargyl amine.[38] We conducted click reactions in oxygen-free DMSO at 50 °C with copper sulfate pentahydrate as the catalyst and ascorbic acid as the reductant. To explore reaction efficiency, we used either 2 or 5 equivalents of excess Gal-Alk per azide. Reaction products were analyzed by ATR−FTIR for evidence of consumption of the azide group at 2107 nm and by ^{1}H NMR for evidence of triazole (Tz) formation. Representative products were also

https://doi.org/10.1021/acspolymersau.3c00011
ACS Polym. Au 2023, 3, 383−393

analyzed by SEC/MALS/RI since, after the reaction, solubility in DMF was vastly improved and M_n and dispersity information could be directly obtained (Table 1 and Figure 4C).

The click reactions were remarkably efficient for all substrates and proceeded with 96−99+% efficiency, even for the preparation of fully glycosylated homopolymers ($GalTzp_{35}$) and brush polymers [$(Tzp_{15}$-*s*-$AcPro_{45})$-*g*-$BnGlu_{70}$] (Table 2). Reactions with only 2 equiv of alkyne per azide were also essentially quantitative. We hypothesize that the high efficiency of the click reactions is, in part, due to the helical polypeptide backbone, where azide groups are displayed in a highly ordered and accessible fashion. Similarly, high efficiencies have been observed for click reactions performed on a variety α-helical polypeptides.[23,60,61] Here, we were particularly pleased to achieve high reaction efficiency with the preparation of grafting-to-bottlebrush polymers. Acetyl and Bn groups were readily removed from the polymers post-click, as previously described. All structures were readily soluble in water and were purified by dialysis or spin filtration, and then lyophilized to dryness. We investigated the thermoresponsiveness of the post-click structures, but no LCST was observed (see Supporting Information Table S1).

Table 2. Results of Copper-Catalyzed Click Reactions on Various Azp-Containing Polypeptides

backbone[a]	alkyne[a]	equivs[b]	product	graft %[c]
Azp_{35}	Gal	5	$GalTzp_{35}$	99+
Azp_{35}	EG	5	$EGTzp_{35}$	96
Azp_{15}-*s*-Hyp_{45}	Gal	2	$GalTzp_{15}$-*s*-Hyp_{45}	99+
Azp_{15}-*s*-Hyp_{45}	Gal	5	$GalTzp_{15}$-*s*-Hyp_{45}	99+
Azp_{15}-*s*-Hyp_{45}	Glc	5	$GalTzp_{15}$-*s*-Hyp_{45}	99+
Azp_{15}-*s*-Hyp_{45}	EG	5	$EGTzp_{15}$-*s*-Hyp_{45}	99+
Azp_{15}-*s*-Hyp_{45}	Glu_{70}	5	$(Tzp_{15}$-*s*-$Hyp_{45})$-*g*-Glu_{70}	99+

[a]For the click reaction, Hyp, Gal, and Glc were protected with acetate groups and Glu with benzyl groups. All protecting groups were removed post-click. [b]Equivalents of alkyne per azide. [c]Grafting efficiency as determined by the combination of relative azide vs amide integrations by ATR−FTIR, ^{1}H NMR, and M_n SEC/MALS/RI.

Considering that the 4*R* Az group stabilizes the aqueous PPII helix, we were curious about the structural effects of the Tz group as well as pendent EG, saccharide, and polyelectrolyte chains. Interestingly, we found that the identity of the group appended and the density of spacing affected the wavelength of the n → π^* and $\pi \rightarrow \pi^*$ CD absorbances and their intensities (Figure 5). The spectra for $GalTzp_{15}$-*s*-Hyp_{45} indicated the PPII structure was relatively unchanged from that of the parent polymer backbone.

However, the fully substituted $GalTzp_{35}$ polymer spectra had reduced characteristic PPII absorbances and a new maximum at ca. 197 nm (Figure 5A). $EGTzp_{15}$-*s*-Hyp_{45} had a similar spectrum to $GalTzp_{35}$ with reduced PPII character and a new 196 nm maximum (Figure 5B). $GalTzp_{15}$-*s*-Hyp_{45} and $GlcTzp_{15}$-*s*-Hyp_{45} lacked the ∼196 absorbance and had classic PPII spectra. In all cases, the PPII n → π^* and $\pi \rightarrow \pi^*$ absorbances were slightly reduced, indicating that the 4*R*-Tz group is less favorable for helical packing than the 4*R*-Az group.

PGlu's CD spectra are essentially identical to those of PPro, but absorbances are shifted ∼10 nm.[46,47] Indeed, our data for $PGlu_{70}$ before click-grafting to Azp_{15}-*s*-Hyp_{45} highlights this spectral difference (Figure 5C). Not surprisingly, the post-grafting spectra are dominated by absorbances of the PGlu chains. Interestingly, the $\pi \rightarrow \pi^*$ is drastically increased in intensity.

Hydrogen bonding, and organization of water molecules near the backbone, or other steric factors could be drivers of absorbances. Spectral overlap in the n → π^* and $\pi \rightarrow \pi^*$ absorbances can also convolute these intensities.[50] Clearly, there is more work to be done to understand the various factors that contribute to amide bond absorptions in CD spectroscopy. Collectively, our data offer additional insights into the drivers of the wavelengths and intensities with which amide electronic transitions occur.

Considering the many applications of Pro-based materials in biological systems, we sought to examine the cytocompatibility of a subset of our polymers. To investigate the effects of the Az group, we selected Azp_{15}-*s*-Hyp_{45} vs Hyp_{75}, and we selected post-click $GalTzp_{15}$-*s*-Hyp_{45}. Cytotoxicity was not expected since Azp amino acids have been previously used as chemical reporters of collagen function and were readily consumed by cells and incorporated into proteins.[62] We treated live human embryonic kidney 293 cells with varied concentrations of polymer for 24 h. We then quantitated viable cell numbers using a commercial proliferation and cytotoxicity assay (CCK8 assay). Cells were treated with phosphate buffered saline (PBS) as a negative control and Triton X-100 as a positive

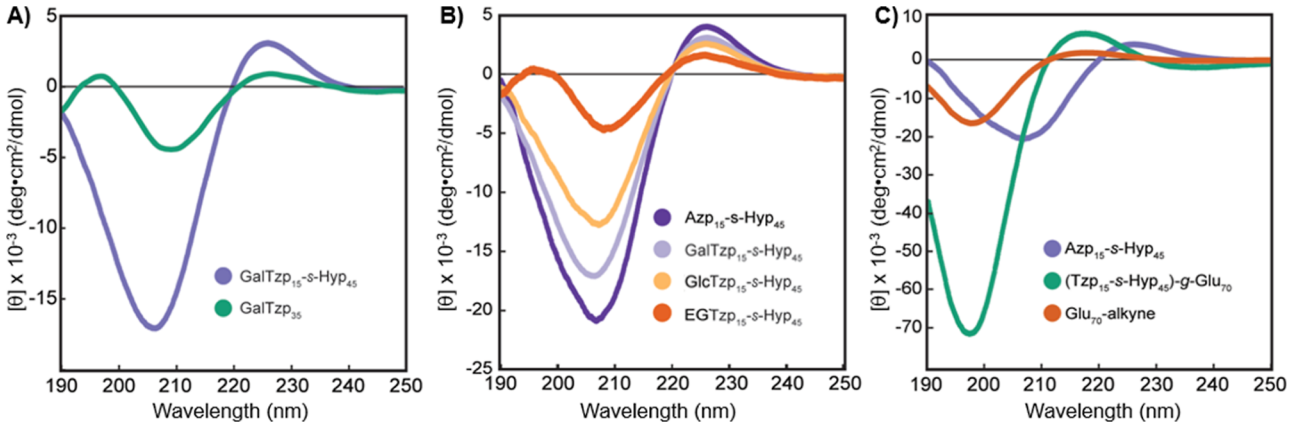

Figure 5. Aqueous CD spectra at 20 °C of (A) Gal clicked homo- and co-Tzp polymers; (B) Tzp_{15}-*s*-Hyp_{45} backbones before and after grafting of various sugars and monomethyl EG; (C) Glu_{70} and Tzp_{15}-*s*-Hyp_{45} backbones before click grafting, and polyelectrolyte bottlebrushes.

https://doi.org/10.1021/acspolymersau.3c00011
ACS Polym. Au 2023, 3, 383−393

control. Data were analyzed via a Tukey test, and there were no statistical differences between the PBS control and any of our polymers, even at the highest concentration tested (Figure 6).

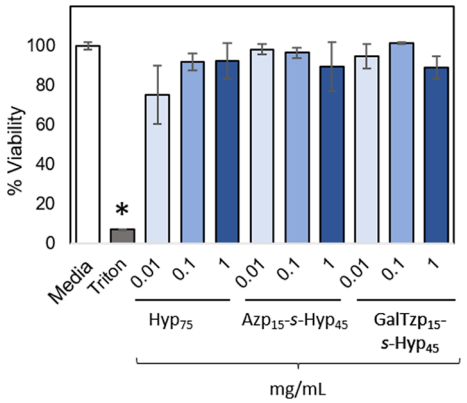

Figure 6. Cell viability and proliferation assay in HEK293 cells after treatment with various concentrations of Hyp_{75}, Azp_{15}-*s*-Hyp_{45}, and $GalTzp_{15}$-*s*-Hyp_{45}. Media and Triton are negative and positive controls, respectively. Data were collected in triplicate and are represented as mean ± SEM, and * represents statistical significance.

In conclusion, we utilized rapid and scalable NCA polymerization to prepare clickable helical polypeptides based on azido-proline residues. The NCA method allowed the generation of tunable high MW homopolymers as well as block and statistical copolymers. We studied the conformational effects of azidoproline residues and found that in water, the PPII helix is stabilized. In organic solvents, it appears that the conformation is shifted toward the PPI helix. Polypeptide LCST could also be tuned by varying the azido-proline content. We utilized the azide groups in high-efficiency click reactions to install EG or saccharides and in the preparation of polyelectrolyte brushes. The backbone and post-click polymers were well tolerated by human cells. Our clickable polypeptides are envisioned to find widespread application to tune the function of polyprolines in mimics of mucins, collagen, and other extracellular matrix components.

METHODS

Instrumentation and General Methods

Full details on instrumentation can be found in the Supporting Information. Reactions were conducted under an inert atmosphere of N_2, using oven-dried glassware unless otherwise stated. Hexanes and dichloromethane were purified by first purging with dry nitrogen, followed by passage through columns of activated 3 Å molecular sieves. THF was purified by first purging with dry nitrogen, followed by passage through columns of activated alumina. Commercial anhydrous DMF was purchased and stored over 3 Å molecular sieves. All oven-dried glassware was dried at 120 °C. For Azp_{15}-*s*-$AcOPro_{45}$, a d*n*/d*c* used was 0.083. For glycosylated samples, a d*n*/d*c* of 0.045 was used. Data for ^{1}H NMR are reported as follows: chemical shift (δ ppm), multiplicity, coupling constant (Hz), and integration. Data for ^{13}C NMR spectra are reported in chemical shift.

4*R*-Azido-L-proline NCA (Azp NCA)

Azp (0.9 g, 3.51 mmol, 1.0 equiv) was suspended in 35 mL of anhydrous THF. The AA, reaction vessel, and stir bar were dried under vacuum overnight. Triphosgene (0.52 g, 1.76 mmol, 0.5 equiv) was added as a crystalline solid to the suspension. Reaction was placed on an ice bath. After 15 min, distilled triethylamine (0.39 g, 3.86 mmol, 1.1 equiv) was added slowly. The reaction was stirred for 2 h under N_2 at RT and monitored by ATR−FTIR. Triethylamine·HCl salts were filtered off with cotton, and the remaining phosgene and solvent were evaporated under reduced pressure and sequestered in a tandem solvent trap system cooled by liquid N_2. Traps were subsequently quenched with ammonium hydroxide. The crude Azp NCA was purified by anhydrous silica chromatography[37] using anhydrous THF and hexanes as the solvent system for elution where 2 column volumes each 25, 35, and 45% THF in hexanes as the gradient. Fractions were analyzed by TLC, followed by ATR−FTIR. Fractions containing only NCA were combined and condensed to give pure Azp NCA (54% yield) as a white crystalline solid. ^{1}H NMR (400 MHz, $CDCl_3$): δ 4.55 (dd, J = 10.9, 6.4 Hz, 2H), 4.03 (dd, J = 12.5, 6.0 Hz, 1H), 3.34 (dd, J = 12.5, 2.1 Hz, 1H), 2.42 (dd, J = 13.4, 6.6 Hz, 1H), 2.12 (ddd, J = 13.4, 10.5, 5.9 Hz, 1H). ^{13}C NMR (500 MHz, $CDCl_3$) 167.46, 154.40, 62.66, 61.84, 52.46, 34.55.

General Procedure for Preparation of PAzp with Benzylamine

The preparation of PAzp was performed based on a literature procedure.[38] All polymerization reactions were performed open to air, at ambient temperature. NCAs were dissolved in DMSO with 5% water at 100 mg/mL. Benzylamine was added in one shot via syringe at the desired monomer-to-initiator ratio. Reaction progress was monitored by ATR−FTIR, where NCA carbonyl absorbances disappeared and amide bonds appeared. See Section SV, Figure S5 for representative IR spectra. Polymerizations were generally complete within 1 h.

General Procedure for Preparation of PAzp and PAcOPro or PPro Copolymers with Nickel Catalyst

The preparation of nickel catalyst as shown in Scheme 1 was performed according to a literature procedure.[63] All polymerization reactions were performed in an N_2-filled glove box. NCAs were dissolved in DMF at 50 mg/mL. 1 was added in one shot via syringe at the desired monomer-to-initiator ratio. The reaction was removed from the glovebox in a bomb tube and heated at 50 °C, and polymerization progress was monitored by ATR−FTIR, where NCA carbonyl absorbances disappeared and amide bonds appeared. See Section SV, Figure S6 for representative IR spectra. Polymerizations were generally complete overnight. Reactions were precipitated into 1 mM HCl in diethyl ether (pH ∼ 3) to remove nickel species. Polymers were collected by centrifugation and dried under reduced pressure to give PAzp statistical copolymers in an essentially quantitative yield. The length characterization of $PAzp_{0.25}$-stat-$PAcOP_{0.75}$ by GPC used the d*n*/d*c* value found for PAcOP of 0.083, as calculated mass recovery was nearly 100%.

General Procedure for Block Copolymers Using $(PMe_3)_4Co$

BnGlu NCA was dissolved in anhydrous THF inside an N_2 filled glove box at a concentration of 50 mg/mL. A 30 mg/mL solution of $(PMe_3)_4Co$ in anhydrous THF was added to the NCA solution at [M]/[I] = 25. All NCA was consumed and converted to polyBnGlu (PBnGlu) within 1 h as evidenced by ATR−FTIR. The PBG solution was used as a macroinitiator to make block copolymers with PAzp. Azp NCA was dissolved in THF at 50 mg/mL. The PBnGlu was added at the desired [M]/[I]. These diblock copolymers were heated in bomb tubes outside of the glovebox at 50 °C. All NCA was consumed overnight. See Section SV, Figure S7.

General Procedure for Statistical Copolymers

Copolymers were synthesized with a $(PMe_3)_4Co$ catalyst. NCAs were dissolved in either DMF or THF at concentrations of 50 mg/mL. NCAs were mixed at the desired ratio. The catalyst was added in one shot via syringe at the desired monomer-to-initiator ratio. Polymerizations were complete within 1−3 h, as evidenced by ATR−FTIR.

General Procedure for Preparation of PBnGlu with Propargylamine

Preparation of PBnGlu was performed based on a literature procedure.[38] All polymerization reactions were performed open to

https://doi.org/10.1021/acspolymersau.3c00011
ACS Polym. Au 2023, 3, 383−393

air, at ambient temperature. NCAs were dissolved in THF with water (to make 5% including water in the initiator solution) at 100 mg/mL. Propargylamine (25× dilution in water) was added in one shot via syringe at the desired monomer-to-initiator ratio. Reaction progress was monitored by ATR−FTIR, where NCA carbonyl absorbances disappeared and amide bonds appeared. Polymerizations were complete within 1 h.

General Procedure for Copper Click Reactions

Azide-functionalized polyproline (1 equiv per azide, 6.1 mg at 25 mol % Azp, 1.09×10^{-5} mol), Gal-alkyne (31.3 mg, 5 equiv, 5.43×10^{-5} mol), $Cu_2SO_4{\cdot}5H_2O$ (0.1 equiv, 0.27 mg, 1.09×10^{-6} mol), PMDETA (0.1 equiv, 0.19 mg, 0.23 μL, 1.09×10^{-6} mol), and solvated DMSO/water = 9:1 (0.1 M, 540 μL) were added to a flask. The reaction was degassed three times with freeze−pump−thaw cycles. The flask was opened to quickly add ascorbic acid (0.5 equiv), and then five more freeze−pump−thaw cycles were performed with N_2 backfilling each time. The reaction was mixed under N_2 at 50 °C for 48 h, then quenched by exposure to air. The click product was deprotected and purified using spin filtration (MWCO 3 kDa). See SI for representative ATR−FTIR spectra.

General Procedure for Deacetylation of Polymers Containing AcOPro or Acetylated Sugars

Polymer was suspended in 0.25 M K_2CO_3 (5 equiv per AcO group) in H_2O or 1:1 = MeOH/H_2O and stirred overnight. Polymer solids had dissolved after ∼16 h. The solution was transferred to 3 kDa cut-off spin filters and centrifuged three times with deionized water or 1:1 = MeOH/H_2O, depending on polymer solubility. The solution was recovered, and residual methanol was evaporated, frozen, and lyophilized to afford a white foam. See Supporting Information for representative ATR−FTIR spectra.

General Procedure for Debenzylation of $PBnGlu_{70}$ Brush Polymers

Deprotection was performed based on a literature procedure.[64] Polymer solids (600 mg, 2.75 moles of benzyl group) were dissolved in DCM. To this solution, distilled TMSI (at least 6 equiv per benzyl group, 2.4 mL, 0.0169 mol) was added via syringe under a stream of N_2, forming a red-brown solution. The reaction was stirred at room temperature for 24 h. The solution was concentrated under vacuo. Saturated $NaHCO_3$ solution (10 mL) and DI water (10 mL) were added to dissolve the resulting residue, and NaS_2O_3 was added until the solution was colorless (6 mL). This was allowed to stir at room temperature for 24 h, resulting in a white, milky solution. The solution was washed 3 × 30 mL with ether. The final product was purified by dialysis (MWCO 12 kDa) against DI water and then lyophilized.

■ ASSOCIATED CONTENT

Supporting Information

The Supporting Information is available free of charge at https://pubs.acs.org/doi/10.1021/acspolymersau.3c00011.

Full experimental details, characterization of compounds, instrumentation, and additional data (PDF)

■ AUTHOR INFORMATION

Corresponding Author

Jessica R. Kramer − *Department of Biomedical Engineering, University of Utah, Salt Lake City, Utah 84112, United States; Department of Molecular Pharmaceutics, University of Utah, Salt Lake City, Utah 84112, United States;* orcid.org/0000-0002-4268-0126; Email: jessica.kramer@utah.edu

Authors

Rachel E. Detwiler − *Department of Biomedical Engineering, University of Utah, Salt Lake City, Utah 84112, United States*

Thomas J. McPartlon − *Department of Molecular Pharmaceutics, University of Utah, Salt Lake City, Utah 84112, United States*

Clara S. Coffey − *Department of Biomedical Engineering, University of Utah, Salt Lake City, Utah 84112, United States*

Complete contact information is available at: https://pubs.acs.org/10.1021/acspolymersau.3c00011

Author Contributions

The manuscript was written through contributions of all authors. All authors have given approval to the final version of the manuscript. CRediT: **Rachel E Detwiler** conceptualization (equal), data curation (equal), formal analysis (equal), methodology (equal), visualization (equal), writing-original draft (equal), writing-review & editing (equal); **Thomas J Mcpartlon** data curation (equal), formal analysis (equal), methodology (equal), writing-review & editing (equal); **Clara S Coffey** data curation (equal), formal analysis (equal), methodology (equal), writing-review & editing (supporting).

Funding

Prof. Jessica Kramer acknowledges financial support from USA NIH NIGMS 1R35GM147262-01, USA NSF DMR-1848054. Clara Coffey acknowledges financial support from the University of Utah Undergraduate Research Opportunity Program.

Notes

The authors declare no competing financial interest.

■ ACKNOWLEDGMENTS

We thank the laboratory of Prof. Michael Yu for the use of their circular dichroism spectrometer.

■ ABBREVIATIONS

PP	polyproline
NMR	nuclear magnetic resonance
ATR−FTIR	attenuated total reflectance infrared spectroscopy
CD	circular dichroism
DMF	dimethylformamide
THF	tetrahydrofuran
NCA	*N*-carboxyanhydride

■ REFERENCES

(1) Shoulders, M. D.; Raines, R. T. Collagen Structure and Stability. *Annu. Rev. Biochem.* **2009**, *78*, 929−958.

(2) Corfield, A. P. Mucins: A biologically relevant glycan barrier in mucosal protection. *Biochim. Biophys. Acta, Gen. Subj.* **2015**, *1850*, 236−252.

(3) Siligardi, G.; Drake, A. F. The Importance of Extended Conformations and, in Particular, the PII Conformation for the Molecular Recognition of Peptides. *Biopolymers* **1995**, *37*, 281−292.

(4) Adzhubei, A. A.; Sternberg, M. J. E.; Makarov, A. A. Polyproline-II Helix in Proteins: Structure and Function. *J. Mol. Biol.* **2013**, *425*, 2100−2132.

(5) Traub, W.; Shmueli, U. Structure of Poly-L-Proline I. *Nature* **1963**, *198*, 1165−1166.

(6) Ramachandran, G. N.; Ramakrishnan, C.; Sasisekharan, V. Stereochemistry of Polypeptide Chain Configurations. *J. Mol. Biol.* **1963**, *7*, 95−99.
(7) Cowan, P. M.; McGavin, S.; North, A. C. T.; Bruno, L. The Polypeptide Chain Configuration of Collagen. *J. Chem. Inf. Model.* **1955**, *176*, 1062−1064.
(8) Steinberg, I. Z.; Harrington, W. F.; Berger, A.; Sela, M.; Katchalski, E. The Configurational Changes of Poly-L-Proline in Solution. *J. Am. Chem. Soc.* **1960**, *82*, 5263−5279.
(9) Harrington, W. F.; Sela, M. Studies on the Structure of Poly-l-Proline in Solution. *BBA, Biochim. Biophys. Acta* **1958**, *27*, 24−41.
(10) Kurtz, J.; Berger, A.; Katchalski, E. Mutarotation of Poly-L-Proline. *Nature* **1956**, *178*, 1066−1067.
(11) Steinberg, I. Z.; Berger, A.; Katchalski, E. Reverse Mutarotation of Poly-l-Proline. *BBA, Biochim. Biophys. Acta* **1958**, *28*, 647−648.
(12) Dukor, R. K.; Keiderling, T. A. Mutarotation Studies of Poly-L-Proline Using FTIR, Electronic and Vibrational Circular Dichroism. *Biospectroscopy* **1998**, *2*, 83−100.
(13) Detwiler, R. E.; Schlirf, A. E.; Kramer, J. R. Rethinking Transition Metal Catalyzed N-Carboxyanhydride Polymerization: Polymerization of Pro and AcOPro N-Carboxyanhydrides. *J. Am. Chem. Soc.* **2021**, *143*, 11482−11489.
(14) Schuler, B.; Lipman, E. A.; Steinbach, P. J.; Kumke, M.; Eaton, W. A. Polyproline and the "Spectroscopic Ruler" Revisited with Single-Molecule Flourescence. *Proc. Natl. Acad. Sci. U.S.A.* **2005**, *102*, 2754−2759.
(15) Gkikas, M.; Avery, R. K.; Olsen, B. D. Thermoresponsive and Mechanical Properties of Poly(L-Proline) Gels. *Biomacromolecules* **2016**, *17*, 399−406.
(16) Sato, S. I.; Kwon, Y.; Kamisuki, S.; Srivastava, N.; Mao, Q.; Kawazoe, Y.; Uesugi, M. Polyproline-Rod Approach to Isolating Protein Targets of Bioactive Small Molecules: Isolation of a New Target of Indomethacin. *J. Am. Chem. Soc.* **2007**, *129*, 873−880.
(17) Kawasaki, T.; Komai, T. Poly(O-acyl Hydroxy L-proline) (II) Wetting Characteristics and Blood Clotting on Surfaces of Poly O-acetyl, Butyryl, Hexanoyl, Dodecanoyl, and Benzoyl Hydroxy L-proline. *J. Biomed. Mater. Res.* **1985**, *19*, 851−861.
(18) Judge, N.; Georgiou, P. G.; Bissoyi, A.; Ahmad, A.; Heise, A.; Gibson, M. I. High Molecular Weight Polyproline as a Potential Biosourced Ice Growth Inhibitor: Synthesis, Ice Recrystallization Inhibition, and Specific Ice Face Binding. *Biomacromolecules* **2023**, *24*, 2459−2468.
(19) Maoz, A.; Fuchs, S.; Sela, M. Immune Response to the Collagen-like Synthetic Ordered Polypeptide (L-Pro-Cly-L-Pro)N. *Biochemistry* **1973**, *12*, 4238−4245.
(20) Lu, H.; Wang, J.; Song, Z.; Yin, L.; Zhang, Y.; Tang, H.; Tu, C.; Lin, Y.; Cheng, J. Recent Advances in Amino Acid N-Carboxyanhydrides and Synthetic Polypeptides: Chemistry, Self-Assembly and Biological Applications. *Chem. Commun.* **2014**, *50*, 139−155.
(21) Huesmann, D.; Klinker, K.; Barz, M. Orthogonally Reactive Amino Acids and End Groups in NCA Polymerization. *Polym. Chem.* **2017**, *8*, 957−971.
(22) Deming, T. J. Synthesis of Side-Chain Modified Polypeptides. *Chem. Rev.* **2016**, *116*, 786−808.
(23) Clauss, Z. S.; Kramer, J. R. Design, Synthesis and Biological Applications of Glycopolypeptides. *Adv. Drug Delivery Rev.* **2021**, *169*, 152−167.
(24) Kramer, J. R.; Deming, T. J. Preparation of Multifunctional and Multireactive Polypeptides via Methionine Alkylation. *Biomacromolecules* **2012**, *13*, 1719−1723.
(25) Rhodes, A. J.; Deming, T. J. Soluble, Clickable Polypeptides from Azide-Containing N-Carboxyanhydride Monomers. *ACS Macro Lett.* **2013**, *2*, 351−354.
(26) Tang, H.; Zhang, D. General Route toward Side-Chain-Functionalized r-Helical Polypeptides. *Biomacromolecules* **2010**, *11*, 1585−1592.
(27) Sonntag, L. S.; Schweizer, S.; Ochsenfeld, C.; Wennemers, H. The "Azido Gauche Effect"—Implications for the Conformation of Azidoprolines. *J. Am. Chem. Soc.* **2006**, *128*, 14697−14703.
(28) Kümin, M.; Sonntag, L. S.; Wennemers, H. Azidoproline Containing Helices: Stabilization of the Polyproline II Structure by a Functionalizable Group. *J. Am. Chem. Soc.* **2007**, *129*, 466−467.
(29) Gorres, K. L.; Raines, R. T. Prolyl 4-Hydroxylase. *Crit. Rev. Biochem. Mol. Biol.* **2010**, *45*, 106−124.
(30) Ganguly, H. K.; Basu, G. Conformational Landscape of Substituted Prolines. *Biophys. Rev.* **2020**, *12*, 25−39.
(31) Shoulders, M. D.; Kotch, F. W.; Choudhary, A.; Guzei, I. A.; Raines, R. T. The Aberrance of the 4 S Diastereomer of 4-Hydroxyproline. *J. Am. Chem. Soc.* **2010**, *132*, 10857−10865.
(32) Inouy, K.; Sakakibara, S.; Prockop, D. J. Effects of the Stereo-Configuration of the Hydroxyl Group in 4-Hydroxyproline on the Triple-Helical Structures Formed by Homogeneous Peptides Resembling Collagen. *BBA, Protein Struct.* **1976**, *420*, 133−141.
(33) Horng, J.; Raines, R. T. Stereoelectronic Effects on Polyproline Conformation. *Protein Sci.* **2006**, *15*, 74−83.
(34) Seo, J.; Martásek, P.; Roman, L. J.; Silverman, R. B. Selective L-Nitroargininylaminopyrrolidine and l-Nitroargininylaminopiperidine Neuronal Nitric Oxide Synthase Inhibitors. *Bioorg. Med. Chem.* **2007**, *15*, 1928−1938.
(35) Gkikas, M.; Iatrou, H.; Thomaidis, N. S.; Alexandridis, P.; Hadjichristidis, N. Well-Defined Homopolypeptides, Copolypeptides, and Hybrids of Poly(l-Proline). *Biomacromolecules* **2011**, *12*, 2396−2406.
(36) Wilder, R.; Mobashery, S. The Use of Triphosgene in Preparation of N-Carboxy α-Amino Acid Anhydrides. *J. Org. Chem.* **1992**, *57*, 2755−2756.
(37) Kramer, J. R.; Deming, T. J. General Method for Purification of α-Amino Acid-N-Carboxyanhydrides Using Flash Chromatography. *Biomacromolecules* **2010**, *11*, 3668−3672.
(38) Hu, Y.; Tian, Zi-Y.; Xiong, W.; Wang, D.; Zhao, R.; Xie, Y.; Song, Y. Q.; Zhu, J.; Lu, H. Water-Assisted and Protein-Initiated Fast and Controlled Ring-Opening Polymerization of Proline N-Carboxyanhydride. *Natl. Sci. Rev.* **2022**, *9*, nwac033.
(39) Cheng, J.; Deming, T. J. Synthesis of Polypeptides by Ring-Opening Polymerization of α-Amino Acid N-Carboxyanhydrides. *Topics in Current Chemistry*; Springer Berlin Heidelberg, 2012.
(40) Kricheldorf, H. R. Polypeptides and 100 Years of Chemistry of α-Amino Acid N-Carboxyanhydrides. *Angew. Chem., Int. Ed.* **2006**, *45*, 5752−5784.
(41) González-Henríquez, C. M.; Sarabia-Vallejos, M. A.; Rodríguez-Hernández, J. Strategies to Fabricate Polypeptide-Based Structures via Ring-Opening Polymerization of N-Carboxyanhydrides. *Polymers* **2017**, *9*, 551.
(42) Lv, W.; Wang, Y.; Li, M.; Wang, X.; Tao, Y. Precision Synthesis of Polypeptides via Living Anionic Ring-Opening Polymerization of N-Carboxyanhydrides by Tri-Thiourea Catalysts. *J. Am. Chem. Soc.* **2022**, *144*, 23622−23632.
(43) Deming, T. J. Facile Synthesis of Block Copolypeptides of Defined Architecture. *Nature* **1997**, *390*, 386−389.
(44) Deming, T. J.; Curtin, S. A. Chain Initiation Efficiency in Cobalt- and Nickel-Mediated Polypeptide Synthesis. *J. Am. Chem. Soc.* **2000**, *122*, 5710−5717.
(45) Clauss, Z. S.; Kramer, J. R. Polypeptoids and Peptoid-Peptide Hybrids by Transition Metal Catalysis. *ACS Appl. Mater. Interfaces* **2022**, *14*, 22781−22789.
(46) Tiffany, M. L.; Krimm, S. New Chain Conformations of Poly(Glutamic Acid) and Polylysine. *Biopolymers* **1968**, *6*, 1379−1382.
(47) Krimm, S.; Tiffany, M. L. The Circular Dichroism Spectrum and Structure of Unordered Polypeptides and Proteins. *Isr. J. Chem.* **1974**, *12*, 189−200.
(48) Woody, R. W. Optical Rotatory Properties Of Biopolymers. *J. Polym. Sci., Part D: Macromol. Rev.* **1977**, *12*, 181−320.
(49) Rucker, A. L.; Creamer, T. P. Polyproline II Helical Structure in Protein Unfolded States: Lysine Peptides Revisited. *Protein Sci.* **2002**, *11*, 980−985.
(50) Woody, R. W. Circular Dichroism Spectrum of Peptides in the Poly(Pro)II Conformation. *J. Am. Chem. Soc.* **2009**, *131*, 8234−8245.

https://doi.org/10.1021/acspolymersau.3c00011
ACS Polym. Au 2023, 3, 383−393

(51) Shi, Z.; Woody, R. W.; Kallenbach, N. R. Is Polyproline II a Major Backbone Conformation in Unfolded Proteins? *Adv. Protein Chem.* **2002**, *62*, 163−240.
(52) Goodman, M.; Toniolo, C.; Falcetta, J. Conformational Aspects of Polypeptide Structure. XXX. Rotatory Properties of Cyclic and Bicyclic Amides. Restricted and Rigid Model Compounds for Peptide Chromophores. *J. Am. Chem. Soc.* **1969**, *91*, 1816−1822.
(53) Woody, R. W.; Tinoco, I. Optical Rotation of Oriented Helices. III. Calculation of the Rotatory Dispersion and Circular Dichroism of the Alpha- and 310-Helix. *J. Chem. Phys.* **1967**, *46*, 4927−4945.
(54) Badreldin, M.; Le Scouarnec, R.; Lecommandoux, S.; Harrisson, S.; Bonduelle, C. Memory Effect in Thermoresponsive Proline-Based Polymers. *Angew. Chem., Int. Ed.* **2022**, *61*, No. e202209530.
(55) Park, S. B.; Sung, M. H.; Uyama, H.; Han, D. K. Poly(Glutamic Acid): Production, Composites, and Medical Applications of the next-Generation Biopolymer. *Prog. Polym. Sci.* **2021**, *113*, 101341.
(56) Inada, Y.; Furukawa, M.; Sasaki, H.; Kodera, Y.; Hiroto, M.; Nishimura, H.; Matsushima, A. Biomedical and Biotechnological Applications of PEG- and PM-Modified Proteins. *Trends Biotechnol.* **1995**, *13*, 86−91.
(57) Bertozzi, C. R.; Rabuka, D. Structural Basis of Glycan Diversity. In *Essentials of Glycobiology*; Varki, A., Cummings, R. D., Esko, J. D., Freeze, H. H., Stanley, P., Bertozzi, C. R., Hart, G. W., Etzler, M. E., Eds.; Cold Spring Harbor Laboratory Press: Cold Spring Harbor: NY, 2009.
(58) Spicer, C. D.; Davis, B. G. Rewriting the Bacterial Glycocalyx via Suzuki−Miyaura Cross-Coupling. *Chem. Commun.* **2013**, *49*, 2747−2749.
(59) Galibert, M.; Renaudet, O.; Boturyn, D.; Dumy, P. Preparation of Peptide and Other Biomolecular Conjugates through Chemoselective Ligations. *Methods Mol. Biol.* **2011**, *751*, 67−79.
(60) Engler, A. C.; Lee, H. I.; Hammond, P. T. Highly Efficient "Grafting onto" a Polypeptide Backbone Using Click Chemistry. *Angew. Chem., Int. Ed.* **2009**, *48*, 9334−9338.
(61) Quadir, M. A.; Martin, M.; Hammond, P. T. Clickable Synthetic Polypeptides—Routes to New Highly Adaptive Biomaterials. *Chem. Mater.* **2014**, *26*, 461−476.
(62) Amgarten, B.; Rajan, R.; Martínez-Sáez, N.; Oliveira, B. L.; Albuquerque, I. S.; Brooks, R. A.; Reid, D. G.; Duer, M. J.; Bernardes, G. J. L. Collagen Labelling with an Azide-Proline Chemical Reporter in Live Cells. *Chem. Commun.* **2015**, *51*, 5250−5252.
(63) Kramer, J. R.; Onoa, B.; Bustamante, C.; Bertozzi, C. R. Chemically Tunable Mucin Chimeras Assembled on Living Cells. *Proc. Natl. Acad. Sci.* **2015**, *112*, 12574−12579.
(64) Baumgartner, R.; Kuai, D.; Cheng, J. Synthesis of Controlled, High-Molecular Weight Poly(l-Glutamic Acid) Brush Polymers. *Biomater. Sci.* **2017**, *5*, 1836−1844.

https://doi.org/10.1021/acspolymersau.3c00011
ACS Polym. Au 2023, 3, 383−393